ELSEVIER

Journal of Chromatography B, 731 (1999) 45–52

JOURNAL OF CHROMATOGRAPHY B

Application of delayed extraction matrix-assisted laser desorption ionization time-of-flight mass spectrometry for analysis of sphingolipids in tissues from sphingolipidosis patients

Takehisa Fujiwaki[a,*], Seiji Yamaguchi[a], Kazuko Sukegawa[b], Tamotsu Taketomi[c]

[a]*Department of Pediatrics, Shimane Medical University, 89-1 Enya-cho, Izumo, Shimane 693-8501, Japan*
[b]*Department of Pediatrics, Gifu University School of Medicine, 40 Tsukasa-machi, Gifu, 500-8705, Japan*
[c]*Department of Biochemistry, Research Center on Aging and Adaptation, Shinshu University School of Medicine, 3-1-1 Asahi, Matsumoto, Nagano 390-8621, Japan*

Abstract

Sphingolipidosis is due to defects in enzymes involved in hydrolysis of sphingolipids. We analyzed sphingolipids in tissues from patients with sphingolipidosis, including Farber disease (FD, acid ceramidase deficiency), Gaucher disease (GD), Niemann–Pick disease type C (NPDC), and GM1-gangliosidosis (GM1G), using delayed extraction matrix-assisted laser desorption ionization time-of-flight mass spectrometry (DE MALDI–TOF–MS). Crude lipids were extracted from about 100 mg wet weight of autopsied tissues, including liver, spleen, cerebrum or cerebellum. After mild alkaline treatment, a sphingolipid fraction was prepared from the crude lipids and analyzed by DE MALDI–TOF–MS. The results were as follows: (a) In FD liver both the ceramide/sphingomyelin and ceramide/monohexosylceramide ratios were significantly high; (b) in both liver and spleen from a GD patient, the glucosylceramide/sphingomyelin ratio was raised; (c) in liver from a NPDC patient, the monohexosylceramide/sphingomyelin ratio was markedly low, suggesting an increase of sphingomyelin; and (d) in all tissues examined in the GM1G patient, GM1-gangliosides or asialo-GM1-gangliosides, that are undetectable in a normal control, were increased. In conclusion, sphingolipids in human tissues could be directly determined by DE MALDI–TOF–MS, with only a small amount of specimens. This method will be useful for the diagnosis and biochemical evaluation of sphingolipidosis patients.

Keywords: Sphingolipidosis

1. Introduction

Matrix-assisted laser desorption ionization (MALDI), first introduced by Karas and Hillenkamp [1,2], is a useful technique for the determination of macromolecules, such as proteins or glycoproteins that have the molecular weights of several hundreds or thousands daltons. Egge et al. reported that MALDI was useful in determine the molecular weight of native or permethylated neutral glycosphingolipids [3]. Furthermore, Juhasz and Costello applied the technique to ganglioside analysis [4,5].

Delayed ion extraction (DE) was recently introduced to matrix-assisted laser desorption ionization time-of-flight mass spectrometry (MALDI–TOF–MS) by PerSeptive Biosystems (Framingham, MA, USA), and dramatically improved the resolution and

*Corresponding author. Tel.: +81-853-20-2219; fax: +81-853-20-2215.

0378-4347/99/$ – see front matter
PII: S0378-4347(99)00190-5

accuracy of mass spectra. Hence, the DE MALDI–TOF–MS enabled to detect isotopically resolved peaks, and recently applied for the precise identification of lysoglycosphingolipids [6,7], lysogangliosides [8], and monosialo- and disialo-gangliosides [9].

Sphingolipidosis is due to deficiencies of lysosomal enzymes involved in the hydrolysis of sphingolipids. In patients with sphingolipidosis, sphingolipids corresponding to the defective enzymes were accumulated in tissues. There have been known 10 kinds of sphingolipidosis. For the diagnosis of such disorders, sphingolipids are analyzed by thin layer chromatography or high-performance liquid chromatography.

Recently, Taketomi et al. reported the usefulness of DE MALDI–TOF–MS in analysis of glycosphingolipids in human brain tissue [10]. We applied this technique to the analysis of sphingolipids in tissues from 4 patients with sphingolipidosis, such as Farber disease (FD), Gaucher disease type 2 (GD), Niemann–Pick disease type C (NPDC) and GM1-gangliosidosis (GM1G). We report here the usefulness of DE MALDI–TOF–MS in detection of sphingolipidosis patients.

2. Experimental procedures

2.1. Case reports of patients and materials

The materials examined were as follows: (a) The liver from a patient with Farber disease (FD), a 2-year-old boy suffering from subcutaneous nodules, joint ankylosis, cholelithiasis and persistent watery diarrhea, whose liver acid ceramidase activity was 31% of the control level [11,12]; (b) the liver and spleen from a patient with Gaucher disease type 2 (GD), a 3-year-old girl diagnosed from a decrease of 4MU-β-glucosidase activity in skin fibroblasts; (c) the liver from a patient with Niemann–Pick disease type C (NPDC), a 4-year-old boy diagnosed with the evidence of impaired cholesterol esterification in skin fibroblasts; and (d) the liver, cerebrum and cerebellum from a patient with GM1-gangliosidosis (GM1G), a 4-year-old boy diagnosed from decreased 4MU-β-galactosidase activity in lymphocytes. The autopsied liver from a patient with Potter syndrome was used as a control.

α-Cyano-4-hydroxycinnamic acid (α-CHCA) and 2,5-dihydroxybenzoic acid (2,5-DHB) used as matrices for MALDI–TOF–MS were purchased from Sigma Chemical (St. Louis, MO, USA). Acetonitrile and trifluoroacetic acid were from Nacalai Tesque (Kyoto). Other reagents were of analytical grade.

2.2. Lipid extraction and preparation of sphingolipids

The extraction and preparation of sphingolipids were performed as described previously [10], and are schematically represented in Fig. 1. In practice, approximately 100 mg wet mass of tissue was homogenized with 10 ml of chloroform–methanol, 2:1 (v/v), ultrasonicated, and then filtrated through filter paper. Total crude lipids were obtained. We added 2.5 ml of water to the filtrate, and then after centrifugation at 3000 *g* for 15 min., the lower phase was dried under a N_2 flow and then treated with 1 ml of 0.1 *M* NaOH in methanol at 55°C for 1 h to decompose glycerophospholipids. After neutralization with 0.2 ml of 1 *M* HCl in methanol, we added one drop of water and 1 ml of hexane, followed by centrifugation at 3000 *g* for 5 min. After the upper phase was removed, the lower phase was evaporated under nitrogen. The residue was then mixed with 0.8

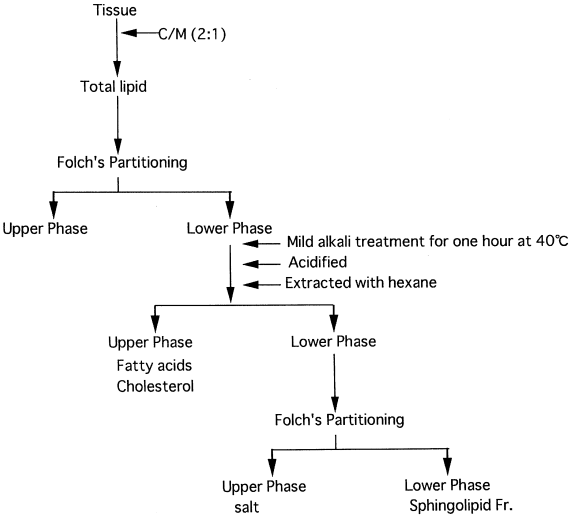

Fig. 1. A diagram for preparation of the sphingolipid fraction.

ml of the theoretical lower phase (chloroform–methanol–water, 86:14:1, v/v/v) and 0.2 ml of the theoretical upper phase (chloroform–methanol–water, 3:48:47, v/v/v) for the Folch partition, and centrifuged the mixture at 3000 *g* for 15 min. After the upper phase was discarded to remove salt, the lower phase was evaporated under a N_2 flow. The residue as crude sphingolipids was dissolved in chloroform–methanol (1:1, v/v) to give a certain concentration for DE MALDI–TOF–MS analysis.

With the above preparation methods, crude alkali-stable sphingolipids were obtained as follows: 2.2 mg, 4.9 mg, 5.9 mg, 5.0 mg, 2.7 mg, 2.7 mg, 3.3 mg, and 1.7 mg of liver from the FD patient, of liver and spleen from the GD patient, of liver from the NPDC patient, liver, cerebrum and cerebellum from the GM1G patient, and control liver, respectively.

2.3. DE MALDI–TOF mass spectrometry

To one and a half microliters of the crude sphingolipid solution in a 1.5 ml Eppendorff tube, 1.5 μl of the matrix solution (10 mg of 2,5-DHB in 1ml of a 9:1 mixture of water–ethanol) was added. The tube was shaken vigorously with a vortex mixer and then centrifuged in a microcentrifuge (Chibitan, Japan Millipore, Tokyo) for 1 min. One microliter of the supernatant obtained was loaded onto a sample plate with 100 sample positions. The plate was loaded into a Voyager™ Elite XL (6.6 m flight length, in reflector mode) Biospectrometry™ Workstation (PerSeptive Biosystems, Framingham, MA, USA), and mass spectra of the samples were obtained in positive or negative ion mode with an N_2 laser (337 nm; laser step: 2300), delay: 100 ns, and scan average: 128. The resolution of the ion peak was more than 2000, as represented with $M/\Delta M$ (peak centroid mass/right mass − left mass), as determined with the resolution calculator in the GRAMS/386 software supplied with the instrument. A two point external calibration was performed each time. In the positive ion mode with 2,5-DHB used as the matrix, potassium ($[M]^+$: 38.9637) and globopentaosylceramide (d18:1C24, $[M+Na]^+$: 1564.9442) were used to calibrate the instrument. In the negative ion mode with 2,5-DHB, lysosulfatide (d18:1, $[M-H]^-$: 540.2843) and GM1 (d18:1C18, $[M-H]^-$: 1544.8689) were used to calibrate the instrument. 5-point Savitsky–Golay smoothing was applied to the mass spectra as described [6–9].

3. Results

The mass numbers and proposed molecular species associated with sphingolipids are shown in Table 1. Mass spectra of sphingolipids obtained by DE MALDI–TOF–MS are presented in Figs. 2–4. In the normal profile sphingolipids from liver as shown in Fig. 2, sphingomyelins corresponding to various molecular weights due to different fatty acid and sphingosine moieties were observed as the major peaks, with several small peaks of monohexosylceramides.

For the liver from the FD patient, as shown in Fig. 3A, peaks of ceramides with different fatty acid carbon numbers, such as *m/z* 616, *m/z* 630 and *m/z*

Table 1
Measured mass to charge ratios (*m/z*) and proposed molecular species associated with sphingolipids

Sphingomyelin		Monohexosylceramide[a]	
m/z		*m/z*	
687	(d18:1C16:1) $[M+H]^+$	722	(d18:1C16) $[M+Na]^+$
697	(d18:1C14) $[M+Na]^+$	738	(d18C17) $[M+Na]^+$
703	(d18:1C16) $[M+H]^+$	750	(d18:1C18) $[M+Na]^+$
725	(d18:1C16) $[M+Na]^+$	764	(d18:1C19) $[M+Na]^+$
727	(d18C16) $[M+Na]^+$	776	(d18:1C20:1) $[M+Na]^+$
731	(d18:1C18) $[M+H]^+$	778	(d18:1C20) $[M+Na]^+$
733	(d18C18) $[M+H]^+$	780	(d18C20) $[M+Na]^+$
741	(d18C17) $[M+Na]^+$	806	(d18:1C22) $[M+Na]^+$
751	(d18:1C18:1) $[M+H]^+$	820	(d18:1C23) $[M+Na]^+$
753	(d18:1C18) $[M+Na]^+$	832	(d18:1C24:1) $[M+Na]^+$
755	(d18C18) $[M+Na]^+$	834	(d18:1C24) $[M+Na]^+$
759	(d18:1C20) $[M+H]^+$	848	(d18:1C25) $[M+Na]^+$
761	(d18C20) $[M+H]^+$		
781	(d18:1C20) $[M+Na]^+$		
783	(d18C20) $[M+Na]^+$		
787	(d18:1C22) $[M+H]^+$		
789	(d18C22) $[M+H]^+$	Ceramide	
807	(d18:1C22:1) $[M+Na]^+$	*m/z*	
809	(d18:1C22) $[M+Na]^+$	616	(d18:1C20) $[M+Na]^+$
811	(d18C22) $[M+Na]^+$	630	(d18:1C21) $[M+Na]^+$
813	(d18:1C24:1) $[M+H]^+$	644	(d18:1C22) $[M+Na]^+$
815	(d18:1C24) $[M+H]^+$		
835	(d18:1C24:1) $[M+Na]^+$		
837	(d18:1C24) $[M+Na]^+$		

[a] Monohexosylceramide includes glucosylceramide.

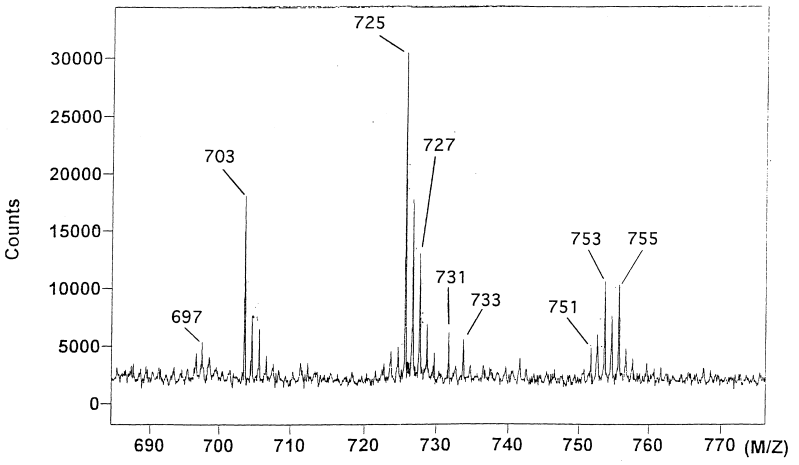

Fig. 2. TOF–MS mass spectra in normal human liver. Measured mass and the proposed molecular species were as follows. m/z 697, sphingomyelin (d18:1C14)$[M+Na]^+$; m/z 703, sphingomyelin (d18:1C16)$[M+H]^+$; m/z 725, sphingomyelin (d18:1C16)$[M+Na]^+$; m/z 727, sphingomyelin (d18C16)$[M+Na]^+$; m/z 731, sphingomyelin (d18:1C18)$[M+H]^+$; m/z 733, sphingomyelin (d18C18)$[M+H]^+$; m/z 751, sphingomyelin (d18:1C18:1)$[M+H]^+$; m/z 753, sphingomyelin (d18:1C18)$[M+Na]^+$; m/z 755, sphingomyelin (d18C18)$[M+Na]^+$ in positive ion mode. Matrix is 2,5-dihydroxy benzoic acid (2,5-DHB).

644, were observed, while undetectable in normal control. The ceramide/sphingomyelin and ceramide/monohexosylceramide intensity ratios were remarkably high, as listed in Table 2. This indicated the accumulation of ceramide in this patient.

In the GD liver, as shown in Fig. 3B, the mass peaks of monohexosylceramides, such as m/z 722, 738 and 750, were apparently elevated. The monohexosylceramide/sphingomyelin intensity ratios were high. This means that monohexosylceramide was accumulated in this patient and that most of the monohexosylceramide was likely to be derived from glucosylceramide, according to the pathogenesis of this disease.

For the liver from the NPDC patient, as shown in Fig. 3C, the mass profile seemingly looked similar to the normal one, being composed of prominent peaks of sphingomyelin and minor ones of monohexosylceramides. In this case, however, the monohexosylceramide/sphingomyelin intensity ratio was extremely low as in Table 1. It was suggested that sphingomyelin was accumulated in this patient, being compatible with the pathogenesis of this disease.

All tissues from the GM1G patient tested had the peaks suggesting GM1-gangliosides (m/z 1517 and 1545) and asialo-GM1-gangliosides (m/z 1277 and 1305), as shown in Fig. 4, while these were undetectable in normal controls.

4. Discussion

The diagnosis of sphingolipidosis has been based on the characteristic clinical features, lipid accumulation in bone marrow cells or rectal mucosa by light microscopy or electron microscopy, abnormalities in lipid analysis of urine or tissues, or defective enzyme activity in cultured cells. However, not a few patients in this field of metabolic disorders of sphingolipids may exhibit atypical manifestations in clinical and biochemical investigation. In such cases, as much as informations from various analytical tools will be of help in the precise identification. We studied the usefulness of DE MALDI–TOF–MS in evaluation of sphingolipids in tissues, using specimens from 4 sphingolipidosis patients.

FD is a deficiency of lysosomal acid ceramidase that hydrolyses ceramide to sphingosine and free fatty acids [13]. In FD patients, accumulation of ceramide is observed in various tissues, and clinically the patients present with multiple subcutaneous periarticular nodules and hoarseness, and often die within the first few years. In our analysis with DE

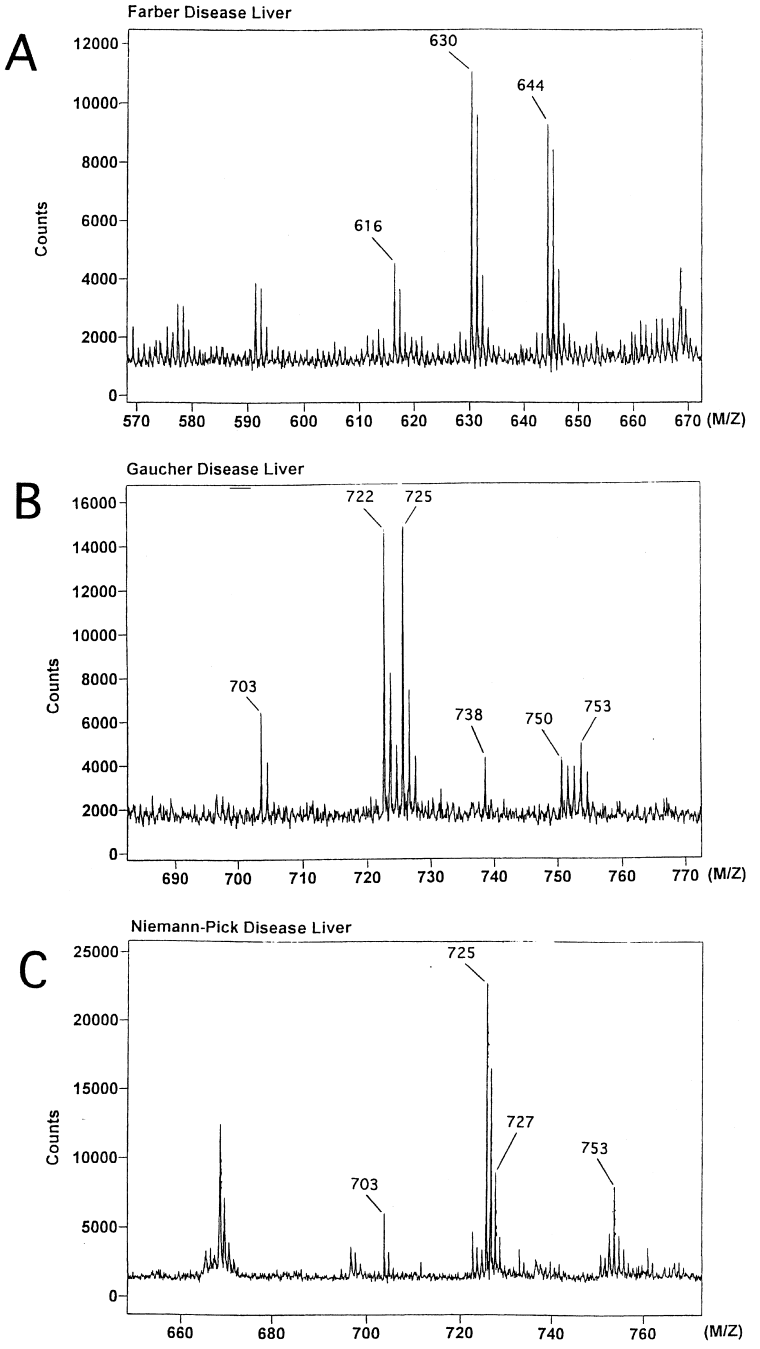

Fig. 3. TOF–MS mass spectra of sphingolipids in liver from patients with Farber disease (A); Gaucher disease (B); and Niemann–Pick disease type C (C). Measured mass and the proposed molecular species were as follows. m/z 616, ceramide (d18:1C20)$[M+Na]^+$; m/z 630, ceramide (d18:1C21)$[M+Na]^+$; m/z 644, ceramide (d18:1C22)$[M+Na]^+$; m/z 703, sphingomyelin (d18:1C16)$[M+H]^+$; m/z 722, monohexosylceramide (d18:1C16)$[M+Na]^+$; m/z 725, sphingomyelin (d18:1C16)$[M+Na]^+$; m/z 738, monohexosylceramide (d18C17)$[M+Na]^+$; m/z 750, monohexosylceramide (d18:1C18)$[M+Na]^+$; m/z 753, sphingomyelin (d18:1C18)$[M+Na]^+$; m/z 727, sphingomyelin (d18C16)$[M+Na]^+$ in positive ion mode. Matrix is 2,5-DHB.

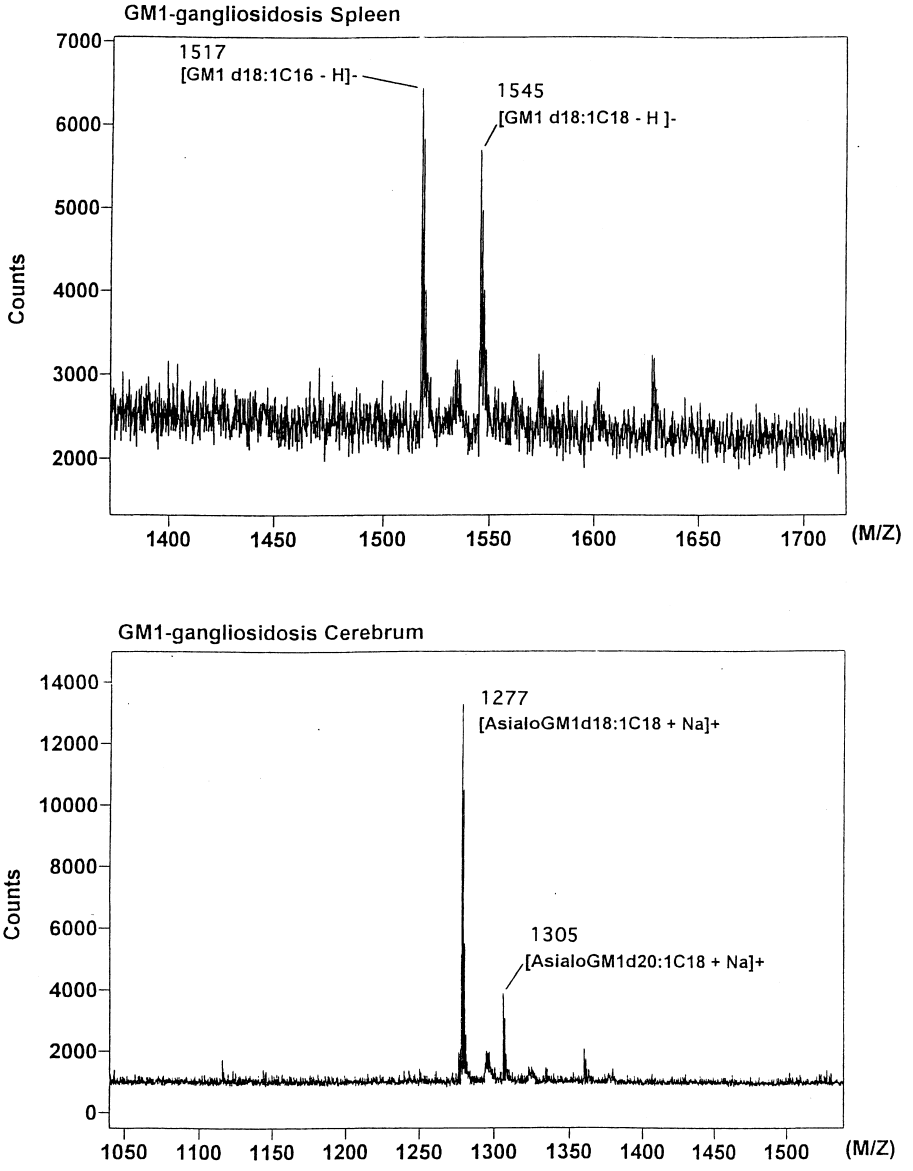

Fig. 4. TOF–MS mass spectra of sphingolipids in a patient with GM1-gangliosidosis. Spleen (upper) and cerebrum (lower). Measured mass and the proposed molecular species were as follows. m/z 1277, asialo GM1-ganglioside (d18:1C18)$[M+Na]^+$; m/z 1305, asialo GM1-ganglioside (d20:1C18)$[M+Na]^+$ in positive ion mode; m/z 1517, GM1-ganglioside (d18:1C16)$[M-H]^-$; m/z 1545, GM1-ganglioside (d18:1C18)$[M-H]^-$ in negative ion mode. Matrix is 2,5-DHB.

MALDI–TOF–MS, a remarkable accumulation of ceramide was revealed.

GD is due to a deficiency of glucocerebrosidase, resulting the accumulation of glucosylceramide in tissues of patients with remarkable hepato-splenomegaly [14]. Three types of GD are delineated: type 1 is most common and characterized by the lack of central nervous system involvement; type 2 is an early onset type and has severe central nervous system involvement and die within the first 2 years of life; type 3 is a late onset and more chronic type with neurologic symptoms. We analyzed

Table 2
Ratios of peak intensities of molecular species of sphingolipids in tissues

Ratio	Cont[a]	FD[a]	GD[a]		NPDC[a]		GM1G[a]		
	Liver	Liver	Liver	Spleen	Liver	Spleen	Liver	Cerebrum	Cerebellum
Ceramide/Sphingomyelin	0.02	0.4	0.00	0.00	0.00	0.00	0.00	0.00	0.00
Ceramide/Monohexosylceramide	0.15	2.88	0.00	0.00	n.d.[b]	n.d.[b]	n.d.[b]	0.00	0.00
Monohexosylceramide/Sphingomyelin	0.17	0.14	0.49[c]	0.79[c]	0.00	0.20	0.21	0.11	0.10

[a] Abbreviations: Cont, control; FD, Farber disease; GD, Gaucher disease; NPDC, Niemann-Pick disease type C; GM1G, GM1-gangliosidosis.
[b] Not determined or only a trace.
[c] Glucosylceramide.

the type 2 GD patient, and detected the raised ratio of peak intensities corresponding to monohexosylceramide to sphingomyelin in liver and spleen. Thinking of the pathogenesis of GD, most of the monohexosylceramide accumulated in this patient may include glucosylceramide. It was suggested by this method that the diagnosis of GD is possible.

NPDC is caused by an error in trafficking of exogenous cholesterol, showing lysosomal accumulation of unesterified cholesterol as well as sphingomyelin [15]. It is clinically characterized by variable hepatosplenomegaly, vertical supranuclear ophthalmoplegia, progressive ataxia, dystonia or dementia, as ''classic manifestations''. In this study, our method revealed an increase of only sphingomyelin in tissues but not cholesterol. The reason why cholesterol was undetectable was that the cholesterol fraction was removed in the sample preparation. Although it was difficult by only this method to distinguish NPDC from the other forms, Niemann–Pick disease type A or B, it was suggested that the accumulation of sphingomyelin in tissues was detectable by this method. Therefore, the disorders that is characterized by the accumulation of sphingomyelin, like Niemann–Pick disease type A, B or C, can be screened at least.

GM1G is due to a deficiency of β-galactosidase with the accumulation of GM1 gangliosides and its asialo derivatives, glycoprotein derived oligosaccharides, and keratan sulfate [16]. Clinically, it is characterized by developmental arrest, neurologic deterioration, generalized spasticity, facial dysmorphism, generalized skeletal dysplasia, hepatomegaly with macular cherry red spots. The accumulation of GM1-gangliosides and asialo-GM1-gangliosides in cerebrum, cerebellum and liver from a 4 year old GM1G patient were clearly detected in this study. It suggested the possibility that GM1G could be simply screened by this method.

It was demonstrated that DE MALDI–TOF–MS would allow the rapid, simple and convenient screening for sphingolipidosis, using only a small amount of tissues. In this study, however, specimens from the autopsied tissues, such as liver, spleen, cerebrum or cerebellum, were used in all cases. To apply this method for the more practical tests, further studies to use more available tissues, such as peripheral lymphocytes or cultured cells, may be required.

References

[1] M. Karas, F. Hillenkamp, Anal. Chem. 60 (1988) 2299.
[2] F. Hillenkamp, M. Karas, Methods Enzymol. 193 (1990) 280.
[3] H. Egge, Pure Appl. Chem. 63 (1991) 491.
[4] P. Juhasz, C.E. Costello, J. Am. Soc. Mass Spectrom. 3 (1992) 785.
[5] C.E. Costelo, P. Juhasz, H. Perreault, Prog. Brain Res. 101 (1994) 45.
[6] T. Taketomi, A. Hara, K. Uemura, E. Sugiyama, J. Biochem. 120 (1996) 573.
[7] T. Taketomi, A. Hara, K. Uemura, H. Kurahashi, E. Sugiyama, Biochem. Biophys. Res. Commun. 224 (1996) 462.
[8] T. Taketomi, A. Hara, K. Uemura, H. Kurahashi, E. Sugiyama, J. Biochem. 121 (1997) 264.
[9] E. Sugiyama, A. Hara, K. Uemura, T. Taketomi, Glycobiology 7 (1997) 719.
[10] T. Taketomi, A. Hara, E. Sugiyama, Proceedings of the Japanese Society for Biomedical Mass Spectrometry, Vol. 22, September 1997, Saga, 1997, p. 21.
[11] T. Fujiwaki, S. Hamanaka, M. Koga, T. Ishihara, R. Nishikomori, E. Kinoshita, K. Furusho, Acta Paediatr. Jpn. 34 (1992) 72.

[12] T. Fujiwaki, S. Hamanaka, S. Tate, F. Inagaki, M. Suzuki, A. Suzuki, C. Mori, Clinica Chimica Acta 234 (1995) 23.
[13] H.W. Moser, in: C.R. Scriver, A.L. Beaudet, W.S. Sly et al. (Eds.), The Metabolic and Molecular Basis of Inherited Diseases, 7th ed, McGraw-Hill, New York, 1995, p. 2589, Ch. 83.
[14] E. Beutler, G.A. Grabowski, in: C.R. Scriver, A.L. Beaudet, W.S. Sly et al. (Eds.), The Metabolic and Molecular Basis of Inherited Diseases, 7th ed, McGraw-Hill, New York, 1995, p. 2641, Ch. 86.
[15] P.G. Pentchev, M.T. Vanier, K. Suzuki, M.C. Patterson, in: C.R. Scriver, A.L. Beaudet, W.S. Sly et al. (Eds.), The Metabolic and Molecular Basis of Inherited Diseases, 7th ed, McGraw-Hill, New York, 1995, p. 2625, Ch. 85.
[16] Y. Suzuki, H. Sakuraba, A. Oshima, in: C.R. Scriver, A.L. Beaudet, W.S. Sly et al. (Eds.), The Metabolic and Molecular Basis of Inherited Diseases, 7th ed, McGraw-Hill, New York, 1995, p. 2785, Ch. 90.